Islamic Azad University

Journal of

Optoelectronical Nanostructures

Summer 2020 / Vol. 5, No. 3

Analysis of Steady-State Brillouin Nonlinearity in High-Power Fiber Lasers

Maryam Ilchi-Ghazaani[*, 1]

[1] Photonics and Quantum Technologies Research School, Nuclear Science and Technology Research Institute (NSTRI), Tehran, Iran

(Received 2 Jun. 2020; Revised 21 Jul. 2020; Accepted 12 Aug. 2020; Published 15 Sep. 2020)

Abstract: In the present work, a theoretical analysis of the first-order of stimulated Brillouin scattering (SBS) in a double-clad (DC) ytterbium (Yb)-doped silica fiber laser in unidirectional pumping mode is presented.

An accurate simulation for calculating SBS nonlinearity is performed by considering the coupled differential rate equations for pump, signal and Stokes powers, as well as population inversion under the initial and boundary conditions in a typical all fiber-based laser with kW-range.

In order to improve the laser operation and increase the laser efficiency, the dependence of different parameters of the laser cavity such as active fiber length, fiber core diameter, dopant concentration, output mirror reflectivity at signal wavelength, as well as the laser linewidth on the Brillouin threshold power has been studied.

In addition, numerical analysis has been compared with the approximate analytical solution presented to emphasize the validity of modeling.

As a result, the proposed laser design can generate up to 2.5 kW of output power without the onset of SBS.

Keywords: Nonlinear Effect, Double-Clad Fibers, Stimulated Brillouin Scattering, Efficiency, Threshold Power, Unidirectional Pumping Mode

1. INTRODUCTION

The advent of DC fiber technology has made it possible to achieve integrated multi-kilowatt high-power lasers with diffraction-limited beam quality. However, the scalability of the output powers can be limited by amplified spontaneous emission (ASE) and nonlinear processes such as stimulated Raman [1-4] and Brillouin [5, 6] scatterings, optical Kerr effect [7], and detrimental thermal barriers.

With the increase in optical power in fiber, the most dominant nonlinearity

* Corresponding author. Email: milchi@aeoi.org.ir

that arises is due to the SBS phenomenon. Although, this nonlinear effect can be considered for specific applications such as slow light, Brillouin fiber ring lasers, and distributed fiber sensors, it can also lead to some unexpected instabilities in high-power fiber lasers or pulse deformation in the fiber amplifiers [5].

In addition, SBS reflects a significant amount of input power to the fiber and limits the amount of transmitted power that can be achieved. It is believed that the maximum power of a CW single-frequency fiber laser amplifier is restricted to several hundred watts due to SBS. SBS reduces the frequency of the incident beam in the opposite direction to the propagation of the main laser beam.

Therefore, the key issue in designing high-power industrial fiber lasers is to estimate the threshold power of the SBS, as well as providing solutions for suppressing destructive Brillouin nonlinearity by optimizing the laser parameters [8-10].

For this purpose, the numerical analysis of the SBS threshold was presented in the linear-cavity Yb-doped fiber laser in 2009 [5]. Moreover, Hekmat et al. investigated the effect of SBS on increasing in the laser output power [6].

Furthermore, this paper theoretically addresses the impact of laser cavity parameters such as pump power, fiber length, core diameter of the active medium, reflection of the output coupler, concentration of dopants as well as laser linewidth on the SBS threshold power. In the next section, the mechanism of Brillouin Stokes and how it manifests in fiber is briefly described. In addition, an approximate analytical expression is extracted to determine the SBS threshold for the first time. Section 3 represents the results of numerical analysis to estimate the Brillouin threshold by solving a set of laser rate equations with SBS. This is followed by the section on conclusions.

These results are expected to provide a guide to the design of co-pumped lasers using all fiber-based configurations.

2. THEORETICAL MODEL

A. Stimulated Brillouin scattering

In the SBS process, a high-coherence narrow linewidth propagating input light interacts with the counter-propagating Stokes wave through electrostriction in an optical fiber, which induces an index grating forms in the fiber due to the longitudinal nature of the acoustic phonons of a crystal lattice [11-13].

As an intermediary, the acoustic wave attenuates the incident light and amplifies the Stokes wave. In other words, the modulation refraction index behaves as an index grating, acting as a moving Bragg grating through the elasto-optic phenomenon, and nonlinear depletion of the incident wave will be occur [14, 15].

Since the scattered light undergoes a Doppler shift, the frequency shift of Brillouin depends on the acoustic velocity and is given by:

$$\nu_B = \frac{2n_{eff}V_a}{\lambda_s} \tag{1}$$

In silica fibers, the velocity of the longitudinal acoustic wave (V_a) within the fiber is 5960 m/s and the effective refractive index (n_{eff}) is equal to 1.444 at the vacuum wavelength of the incident light wave (λ_s).

The strong attenuation of sound waves in silica determines the shape of the Brillouin gain spectrum. Actually, the exponential decay of the acoustic waves leads to a gain, presenting a Lorentzian spectral profile with a full-width at half maximum (FWHM) of ($\Delta\nu_B$) as follows;

$$g_B(\Delta\nu) = g_0 \frac{(\Delta\nu_B/2)^2}{(\nu_B - \nu_s)^2 + (\Delta\nu_B/2)^2} \tag{2}$$

where, $g_B(\Delta\nu)$, denotes the Brillouin gain spectrum peaks at the Brillouin frequency shift, g_0 indicates the intrinsic gain coefficient of Brillouin (peak value), and $\Delta\nu_B$ ascertains the intrinsic Brillouin linewidth [14, 16].

It should be noted that the gain coefficient depends on the material properties, including the acoustic velocity, density and the gain linewidth of Brillouin. In addition, the gain coefficient is reduced at broad spectral linewidths [12].

In the case where the laser linewidth ($\Delta\nu_s$) is much larger than the linewidth of the SBS gain band, the Brillouin gain can be realized as follows [17]:

$$g_B(\Delta\nu) = g_0 \frac{\Delta\nu_B}{\Delta\nu_s + \Delta\nu_B} \tag{3}$$

Conversely, when $\Delta\nu_s \ll \Delta\nu_B$, then $g_B \approx g_0$ which is the maximum gain coefficient in resonance conditions. It is worth mentioning that the fiber material and the numerical aperture affect the SBS linewidth, while the central frequency of the Brillouin Stokes wave is limited by fiber temperature, tension and other parameters [18].

In general, the SBS threshold in a single-mode fiber can be estimated using the following equation [19, 20],

$$P_{SBS} \cong \frac{21A_{eff}}{g_B L_{eff}} = \frac{21A_{eff}}{g_0 L_{eff}}\left(1 + \frac{\Delta\nu_s}{\Delta\nu_B}\right) \tag{4}$$

where, L_{eff} is the effective length of the fiber and A_{eff} represents the effective cross-sectional area of the fiber core that can be written as [21];

$$A_{eff} = \Gamma^2(\frac{\pi}{4})D_{core}^2 \tag{5}$$

Here, Γ is the ratio between the diameter of the mode and that of the fiber core.

B. Rate Equations

The proposed configuration for a typical end-pumped linear-cavity fiber oscillator is shown schematically in Fig. 1, consisting of a Yb-doped fiber, a couple of fiber Bragg grating (FBG), and diode lasers. In this all-fiber integrated structure, the amplifying medium has a length of L with a uniform dopant concentration at the fiber core.

As shown in Fig. 1, the high-reflection FBG with a reflection coefficient of 99.5% at the center line of the laser is located at the front end of the array, and at the end of it, the partial reflector acts as output coupler.

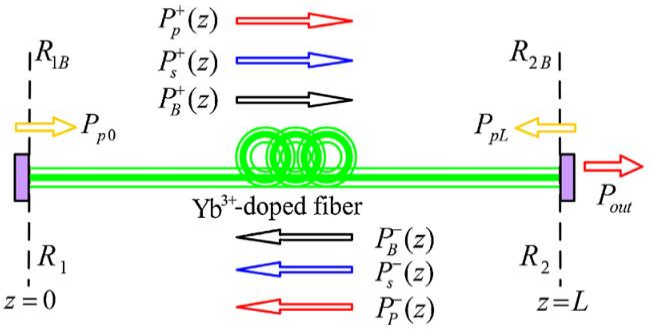

Fig. 1: Schematic illustration of a typical high power CW DC fiber laser with end-pumping

In quasi-three level fiber lasers, time-independent rate equations in steady-state operation are described by the improved model, which are given by equations (9)-(12) as below [22, 23]:

$$\pm\frac{dP_p^{\pm}(z)}{dz} = \pm\Gamma_p[(\sigma_{ap}+\sigma_{ep})N_2(z)-\sigma_{ap}N]P_p^{\pm}(z)\mp\alpha_p P_p^{\pm}(z) \tag{6}$$

$$\pm\frac{dP_s^{\pm}(z)}{dz}=\pm\Gamma_s[(\sigma_{as}+\sigma_{es})N_2(z)-\sigma_{as}N]P_s^{\pm}(z)\mp\alpha_s P_s^{\pm}(z)\pm\Gamma_s\sigma_{es}N_2(z)P_0(\lambda)$$
$$\mp\frac{g_B}{A_{eff}}P_B^{\mp}(z)P_s^{\pm}(z) \quad (7)$$

$$\pm\frac{dP_B^{\pm}(z)}{dz}=\mp\alpha_B P_B^{\pm}(z)\pm\frac{g_B}{A_{eff}}P_s^{\mp}(z)P_B^{\pm}(z) \quad (8)$$

$$\frac{N_2(z)}{N}=\frac{\Gamma_p\lambda_p\sigma_{ap}[P_p^{+}(z)+P_p^{-}(z)]+\Gamma_s\lambda_s\sigma_{as}[P_s^{+}(z)+P_s^{-}(z)]}{\Gamma_p\lambda_p(\sigma_{ap}+\sigma_{ep})[P_p^{+}(z)+P_p^{-}(z)]+\frac{hcA_{eff}}{\tau}+\Gamma_s\lambda_s(\sigma_{as}+\sigma_{es})[P_s^{+}(z)+P_s^{-}(z)]} \quad (9)$$

These equations consist of the coupled nonlinear differential equations relating to pump, signal, first-order steady-state of Brillouin Stokes, and population inversion represented by $P_p^{\pm}(z)$, $P_s^{\pm}(z)$ and $P_B^{\pm}(z)$ accordingly. The ± superscripts denote the propagation direction of optical waves along the coordinate axis (z). Various parameters are introduced in the pump, signal, and Brillouin wavelengths with p, s and B subscripts, respectively.

Here, $N_2(z)$, N and τ show the population inversion of the upper state of atoms, the density of dopants per unit volume and the spontaneous emission lifetime of upper-state atoms, accordingly. The parameters σ_a / σ_e, the dimensionless coefficients Γ_p / Γ_s and α_p / α_s describe the absorption / emission cross-section, pump / signal filling factor, as well as the absorption loss at the pump / signal wavelength, respectively.

The general parameters include Planck's constant (h) and the speed of light in vacuum (c), and the wavelength is indicated by λ. Power density per unit wavelength, $P_0(\lambda)$, is used to determine the contribution of the spontaneous emission in the propagation of the laser transverse mode.

In addition, α_B is the loss of Brillouin scattering. Since the shift of the SBS peak from the center line of the laser is less than 0.2 nm, we can assume that $\alpha_B \approx \alpha_s$ [23].

The two-point boundary conditions that correspond to the above ordinary differential equations can be described as follows;

$$P_p^{+}(0)=\eta_l\times P_p^{+}(tot) \quad (10)$$

$$P_s^{+}(0)=R_1\times P_s^{-}(0) \quad (11)$$

$$P_s^{-}(L)=R_2\times P_s^{+}(L) \quad (12)$$

$$P_B^{+}(0)=R_{1B}\times P_B^{-}(0) \quad (13)$$

$$P_B^-(L) = R_{2B} \times P_B^+(L) \tag{14}$$

where, $P_p^+(tot)$ is the total lunched pump power and η_1 indicates the loss of the pump coupling. Furthermore, R_1 (R_{1B}) and R_2 (R_{2B}) represent the reflectivity of the input and output mirrors at signal (Brillouin Stokes) wavelength, respectively.

The forward and backward Stokes powers are given by;

$$P_B^+(out) = P_B^+(L) - P_B^-(L) = [1 - R_{2B}]\, P_B^+(L) \tag{15}$$

$$P_B^-(out) = P_B^-(0) - P_B^+(0) = [1 - R_{1B}]\, P_B^-(0) \tag{16}$$

C. SBS Threshold Power

As far as one knows, there is no precise analytical solution for SBS distribution in closed form in active fiber lasers because it requires the integration of Stokes waves at different wavelengths across the entire gain bandwidth, which necessitates solving a set of coupled differential equations consist of a great number of two-point boundary value problems (BVPs). This fact draws special attention to numerical solutions to predict the threshold power of the nonlinear SBS for the design of high-power fiber lasers.

However, a semi-analytical technique for determining the SBS threshold is provided here. Initially, the effective fiber length in active fibers is given by;

$$L_{eff} = \frac{\int_0^L P_s^+(z)dz}{P_s^+(0)} \tag{17}$$

Here, $P_s^+(0)$ is the initial value of the forward signal power at z=0. By analytically solving the rate equations [24], we have;

$$P_s^+(z) = \frac{-B + \sqrt{B^2 + 4R_1 P_s^-(0)^2}}{2} \tag{18}$$

where the parameter B can be expressed by;

$$B = P_s^-(0)(1-R_1) + (\frac{\lambda_p}{\lambda_s})(1-\frac{\alpha_p}{\alpha})(1-e^{\alpha z})[\,P_p^+(0)e^{-\alpha z} + P_p^-(L)e^{-\alpha L}\,] + \frac{hCA_{eff}}{\tau\lambda_s}kz \tag{19}$$

In addition, K is a constant parameter as below;

$$K = \frac{\frac{1}{L}\ln(\frac{1}{\sqrt{R_1R_2}}) + (\sigma_{as}\Gamma_s N)}{\Gamma_s(\sigma_{es}+\sigma_{as})} \tag{20}$$

$P_s^-(0)$ is the absolute value of backward signal power at z=0 which is defined by;

$$P_s^-(0) = \frac{\sqrt{R_2}\cdot P_{s,sat}}{\sqrt{R_1}(1-R_2)+\sqrt{R_2}(1-R_1)} \times\left[(\frac{\lambda_p}{\lambda_s})(1-\frac{\alpha_p}{\alpha})(1-e^{-\alpha L})\cdot\frac{P_p^+(0)+P_p^-(L)}{P_{s,sat}} - (\sigma_{as}\Gamma_s N)L - \ln(\frac{1}{\sqrt{R_1R_2}})\right] \tag{21}$$

Moreover, $P_{s,sat}$ shows the signal saturation power as follows;

$$P_{s,sat} \equiv \frac{hCA_{eff}}{\Gamma_s\lambda_s(\sigma_{as}+\sigma_{es})\tau} \tag{22}$$

and, an attenuation coefficient α (in m^{-1}) is given by [25, 26];

$$\alpha = \alpha_p + \Gamma_p\sigma_{ap}N \tag{23}$$

By substituting Eqs. (5) and (17) into Eq. (4), we finally have;

$$P_{SBS} \cong \frac{21A_{eff}}{g_B L_{eff}} = \frac{21\pi}{8}\frac{\Gamma^2 D_{core}^2}{g_0 P_s^+(0)}(1+\frac{\Delta\nu_s}{\Delta\nu_B})\left\{\int_0^L -B + \sqrt{B^2+4R_1P_s^-(0)^2}\,dz\right\}^{-1} \tag{24}$$

Eq. (24) can't be solved analytically. Therefore, the threshold power of SBS should be estimated using an applicable mathematical software. It is found from Eqs. (17)-(24) that the SBS threshold is theoretically related to fiber length, core

diameter, dopant concentration and output coupler reflection, as well as laser and Brillouin linewidths.

3. RESULTS AND DISCUSSION

In the following, the effect of various cavity parameters such as gain length, fiber type with multi-mode cores, dopant concentration and, reflection coefficient of output coupler as well as the laser linewidth on SBS threshold power is investigated in order to mitigate the detrimental Brillouin nonlinearity in high-power fiber lasers.

TABLE 1
THE MAJOR PARAMETERS OF DESIGNED YB:SILICA FIBER LASER

Symbol	Quantity	Value
λ_p	pump wavelength	975×10^{-9} m
σ_{ap}	absorption cross section (@ λ_p)	2.35×10^{-24} m^2
σ_{ep}	emission cross section (@ λ_p)	2.17×10^{-24} m^2
α_p	absorption loss (@ λ_p)	0.003 m^{-1}
Γ_p	pump filling factor	0.0014
λ_s	signal wavelength	1085×10^{-9} m
σ_{as}	absorption cross section (@ λ_s)	6.55×10^{-30} m^2
σ_{es}	emission cross section (@ λ_s)	1.83×10^{-25} m^2
α_s	absorption loss (@ λ_s)	0.005 m^{-1}
Γ_s	signal filling factor	0.82
T	spontaneous lifetime	0.84×10^{-3} s
A_{eff}	effective cross-sectional area	3.14×10^{-10} m^2
N	Yb^{3+} dopant concentration	1.2×10^{26} m^{-3}
L	fiber gain length	15 m
η_1	pump coupling efficiency	0.95
α_B	absorption loss (@ λ_B)	0.005 m^{-2}
g_0	intrinsic SBS gain constant	5×10^{-11} mW^{-2}
$\Delta\nu_s$	laser linewidth	10 GHz
$\Delta\nu_B$	SBS gain linewidth	50 MHz [5]
g_B	SBS gain	2.49×10^{-13} mW^{-2}
R_1	power reflectivity of input-mirror (@ λ_s)	0.995
R_2	power reflectivity of output-mirror (@ λ_s)	0.1
R_{1B}	power reflectivity of input-mirror (@ λ_B)	0.04
R_{2B}	power reflectivity of output-mirror (@ λ_B)	0.04

Rate equations (9)-(12) are solved using the forth-order Rang-Kutta algorithm, as well as the shooting method, taking into account the boundary conditions and applying the initial values of pump, signal and Brillouin powers.

Moreover, numerical analysis has been compared with an approximate analytical solution to emphasize the validation of modeling.

For simplicity, the numerical values of the parameters used in the calculations are tabulated in Table 1.

Fig. 2 shows the variations in the output power of the laser in terms of the incident pump power. As can be seen in the figure, with increasing the pump power up to 632.5 W, the signal output power increases linearly and the laser efficiency remains constant at 66.35%. When the pump power reaches the threshold power of Brillouin, the optical efficiency is greatly reduced and the laser signal will be enhanced negatively. In contrast, the Stokes power has linear growth, and the Brillouin efficiency enhances from zero to 79.7%.

Therefore, the SBS threshold is defined as the power at which the Stokes power is equal to the pump power at the fiber output. In fact, once the input power exceeds the SBS threshold, most of the power is transferred to the backscattered Stokes light, which limits the power of the transmitted signal, and the Stokes power begins to increase significantly.

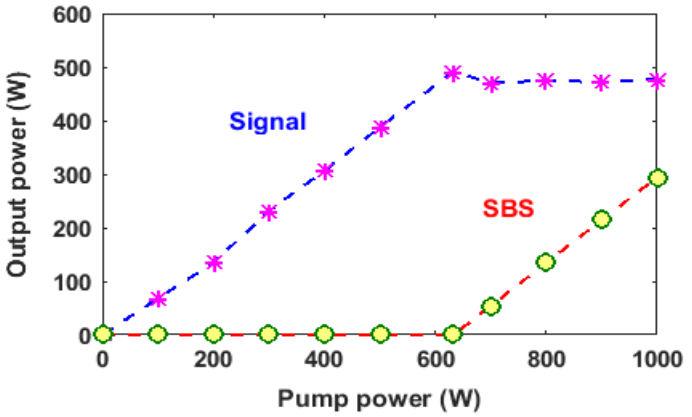

Fig. 2 SBS threshold in fiber laser having 15 m length, 20 μm Core diameter, 1.2×10^{26} m^{-3} dopant concentration at $R_2 = 10\%$ with 10 GHz laser linewidth

Fig. 3 illustrates the simulation results for different fiber lengths at pumping powers up to 2.5 kW. It is evident that the Brillouin threshold power exponentially decreases with increase in length of the fiber. In the range of power under consideration, the SBS threshold is obtained at 2352.2, 979.4,

632.50, 472.32, and 383.44 W for the fiber lengths of 5, 10, 15, 20 and 25 m, respectively.

Consequently, achieving higher output powers and increasing the Brillouin threshold is only possible by reducing the fiber length.

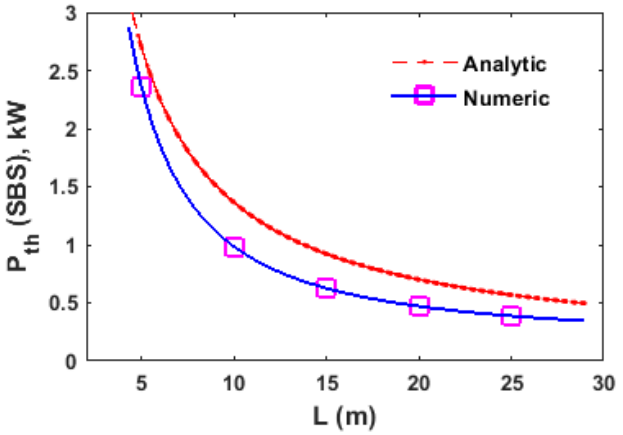

Fig. 3 Effect of fiber length on SBS threshold (D_{core} = 20 μm, N = 1.2×10^{26} m^{-3}, R_2 = 10%, $\Delta\nu_s$ = 10 GHz)

The effect of the diameter of the doped core on the threshold power of Brillouin is shown in Fig. 4. The active fibers used have cores with a diameter of 10, 15, 20, 25 and 30 μm, and SBS is observed at 152.95, 350.47, 632.50, 985.85 and 1425.6 W, accordingly which is in accordance with Eq. (8). Therefore, it is better to use multi-mode LMA fibers in the design of high-power lasers to raise the output power without disturbing the nonlinear effects.

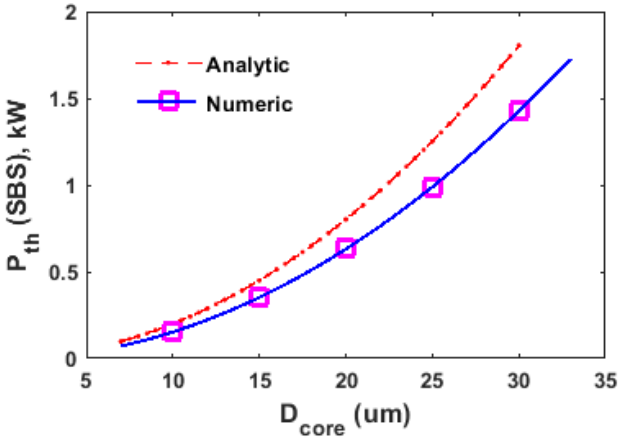

Fig. 4: Estimated SBS threshold versus fiber core diameter (L = 15 m, N =

1.2×10^{26} m^{-3}, $R_2 = 10\%$, $\Delta\nu_s = 10$ GHz)

In addition, the effect of dopant concentration on the growth of Stokes power have been investigated in Fig. 5. A higher depletion in pump power after the Brillouin threshold can be seen at higher concentrations. By lowering the concentration from 2.5×10^{26} m^{-3} to 1.2×10^{25} m^{-3}, the SBS threshold becomes of about 3 times larger.

Therefore, dopant concentration is another factor that can impress the quality of SBS.

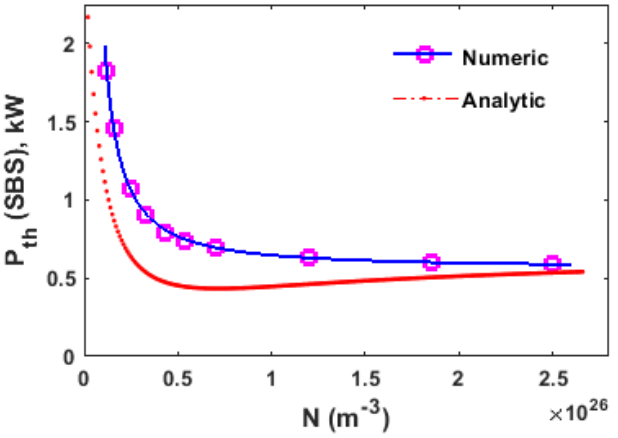

Fig. 5: Effect of dopant concentration on SBS threshold (L = 15 m, D_{core} = 20 μm, $R_2 = 10\%$, $\Delta\nu_s = 10$ GHz)

In the following, Brillouin threshold power is theoretically analyzed under the variation of the output coupler reflection. Regarding Fig. 6, the first-order Stokes wave in the forward pumping does not appear to reach the threshold power of 732.01, 696.22, 661.84, 632.50 and 604.68 W for reflectance of 4%, 6%, 8%, 10% and 12% accordingly.

Meanwhile, the influence of the FBG reflection coefficient on SBS threshold power is less noticeable compared to other laser parameters.

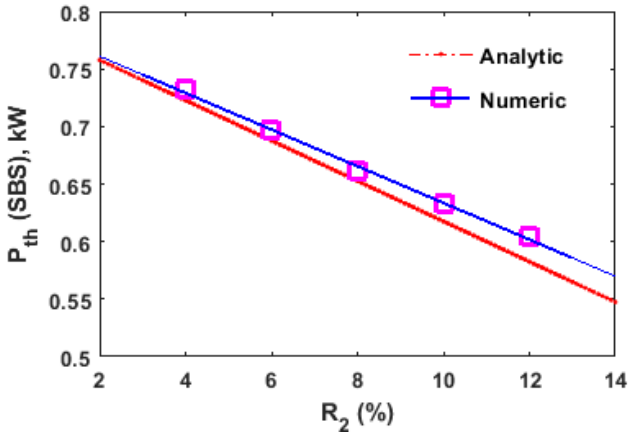

Fig. 6 Estimated SBS threshold versus reflectance coefficient of the output coupler (L = 15 m, D_{core} = 20 μm, N = 1.2×10^{26} m^{-3}, $\Delta\nu_s$ = 10 GHz)

As the last important parameter, the variation of the threshold pump power of inelastic Brillouin scattering in terms of signal linewidth is depicted in Fig. 7. According to this figure, in the range of 1 to 20 GHz, an approximate linear behavior is observed in which the threshold powers of the pump are 7.75 W and 1259.9 W, respectively.

In general, the laser linewidth changes the Brillouin gain according to Eq. (3) so, as the laser linewidth increases, the SBS gain decreases.

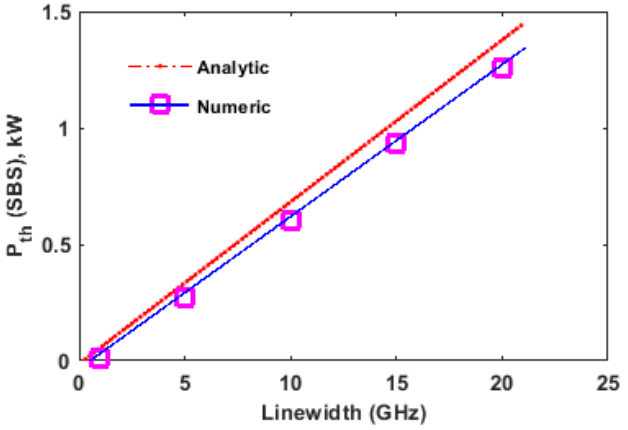

Fig. 7 Effect of the laser linewidth on SBS threshold (L = 15 m, D_{core} = 20 μm, N = 1.2×10^{26} m^{-3}, R_2 = 10%)

4. CONCLUSION

In this work, a typical high-power CW DC fiber laser is designed by taking into account the nonlinear effect of SBS. In addition, the effect of different cavity parameters on the threshold power of Brillouin has been investigated.

Theoretical analysis are performed by numerically solving the differential equations for the pump, the signal, and Stokes powers, and the rate equation for population inversion. In addition, an approximate analytical solution is added to emphasize the validity of modeling.

The results confirm that an alternative to overcoming SBS limitation is to use a large mode area (LMA) fiber (D_{core} = 30 μm), with short active fiber length (L = 5 m), low dopant concentration (N = 1.2×10^{25} m^{-3}) and, low reflection coefficient of the output coupler (R_2 = 4%), as well as high laser linewidth ($\Delta\nu_s$ = 20 GHz).

With such a design, a compact and efficient fiber laser with an output power of up to 2.5 kW can be demonstrated without the onset of SBS.

REFERENCES

[1] Y. Wang, "Dynamics of stimulated Raman scattering in double-clad fiber pulse amplifiers," *Quantum Electronics, IEEE Journal of*, vol. 41, pp. 779-788, 2005.

[2] I. D. Vatnik, D. V. Churkin, S. A. Babin, and S. K. Turitsyn, "Cascaded random distributed feedback Raman fiber laser operating at 1.2 μm," *Optics express*, vol. 19, pp. 18486-18494, 2011.

[3] C.-J. Chen, H. K. Lee, and Y.-J. Cheng, "Instability in Raman amplifiers caused by distributed Rayleigh reflection," in *Optical Fiber Communication Conference*, 2003, p. TuC2.

[4] O. Frazão, C. Correia, J. Santos, and J. Baptista, "Raman fibre Bragg-grating laser sensor with cooperative Rayleigh scattering for strain–temperature measurement," *Measurement Science and Technology*, vol. 20, p. 045203, 2009.

[5] G. Liu and D. Liu, "Numerical analysis of stimulated Brillouin scattering in high-power double-clad fiber lasers," *Optik-International Journal for Light and Electron Optics*, vol. 120, pp. 24-28, 2009.

[6] M. Hekmat, M. Dashtabi, S. Manavi, E. Hassanpour, and R. Massudi, "Study of the stimulated Brillouin scattering power threshold in high power double-clad fiber lasers," *Laser Physics*, vol. 23, p. 025104, 2013.

[7] Y. Wang, C.-Q. Xu, and H. Po, "Analysis of Raman and thermal effects in kilowatt fiber lasers," *Optics communications*, vol. 242, pp. 487-502, 2004.

[8] T. Sakamoto, T. Matsui, K. Shiraki, and T. Kurashima, "SBS suppressed fiber with hole-assisted structure," *Journal of Lightwave Technology*, vol. 27, pp. 4401-4406, 2009.

[9] J. Leng, X. Wang, H. Xiao, P. Zhou, Y. Ma, S. Guo, *et al.*, "Suppressing the stimulated Brillouin scattering in high power fiber amplifiers by dual-single-frequency amplification," *Laser Physics Letters*, vol. 9, p. 532, 2012.

[10] A. Liu, "Novel SBS suppression scheme for high power fiber amplifiers," in *Fiber Lasers III: Technology, Systems, and Applications*, 2006, p. 61021R.

[11] A. Yeniay, J.-M. Delavaux, and J. Toulouse, "Spontaneous and stimulated Brillouin scattering gain spectra in optical fibers," *Journal of lightwave technology*, vol. 20, p. 1425, 2002.

[12] D. Machewirth, V. Khitrov, U. Manyam, K. Tankala, A. Carter, J. Abramczyk, *et al.*, "Large-mode-area double-clad fibers for pulsed and CW lasers and amplifiers," in *Fiber Lasers: Technology, Systems, and Applications*, 2004, pp. 140-150.

[13] H. Al-Asadi, M. Al-Mansoori, M. Ajiya, S. Hitam, M. Saripan, and M. Mahdi, "Effects of pump recycling technique on stimulated Brillouin scattering threshold: A theoretical model," *Optics express*, vol. 18, pp. 22339-22347, 2010.

[14] H. A. Alasadi, M. Al-Mansoori, M. Saripan, and M. Mahdi, "Brillouin linewidth characterization in single mode large effective area fiber through co-pumped technique," *International Journal of Electronics, Computer and Communications Technologies*, vol. 1, pp. 16-20, 2010.

[15] M. Hildebrandt, S. Buesche, P. Weβels, M. Frede, and D. Kracht, "Brillouin scattering spectra in high-power single-frequency ytterbium doped fiber amplifiers," *Optics express*, vol. 16, pp. 15970-15979, 2008.

[16] B. Stiller, M. Delqué, M. W. Lee, S. F. Mafang, J.-C. Beugnot, A. Kudlinski, *et al.*, "Effect of inhomogeneities on backward and forward Brillouin scattering in photonic crystal fibers," in *SPIE Photonics Europe*, 2010, pp. 771406-771406-12.

[17] N. A. Brilliant, "Stimulated Brillouin scattering in a dual-clad fiber amplifier," *JOSA B*, vol. 19, pp. 2551-2557, 2002.

[18] V. I. Kovalev and R. G. Harrison, "Waveguide-induced inhomogeneous spectral broadening of stimulated Brillouin scattering in optical fiber," *Optics letters*, vol. 27, pp. 2022-2024, 2002.

[19] T. Shimizu, K. Nakajima, K. Shiraki, K. Ieda, and I. Sankawa, "Evaluation methods and requirements for the stimulated Brillouin scattering threshold in a single-mode fiber," *Optical Fiber Technology*, vol. 14, pp. 10-15, 2008.

[20] Y. Aoki, K. Tajima, and I. Mito, "Input power limits of single-mode optical fibers due to stimulated Brillouin scattering in optical communication systems," *Lightwave Technology, Journal of*, vol. 6, pp. 710-719, 1988.

[21] J. Zhu, P. Zhou, Y. Ma, X. Xu, and Z. Liu, "Power scaling analysis of tandem-pumped Yb-doped fiber lasers and amplifiers," *Optics express*, vol. 19, pp. 18645-18654, 2011.

[22] M. Ilchi-Ghazaani and P. Parvin, "Distributed scheme versus MOFPA array on the power scaling of a monolithic fiber laser," *IEEE Journal of quantum electronics*, vol. 50, pp. 698-708, 2014.

[23] H. Yang, K. Duan, B. Zhao, and E. Zhang, "Theoretical study of stimulated Brillouin scattering in high-power dual-clad fiber lasers," *Optik-International Journal for Light and Electron Optics*, vol. 124, pp. 1049-1052, 2013.

[24] L. Xiao, P. Yan, M. Gong, W. Wei, and P. Ou, "An approximate analytic solution of strongly pumped Yb-doped double-clad fiber lasers without neglecting the scattering loss," *Optics communications*, vol. 230, pp. 401-410, 2004.

[25] Z. Zhang and H. Gong, "Amplification effect on SBS and Rayleigh scattering in the backward pumped distributed fiber Raman amplifier," *Chinese Optics Letters*, vol. 7, pp. 393-395, 2009.

[26] S. Mohammadian, P. Parvin, M. Ilchi-Ghazaani, R. Poozesh, and K. Hejaz, "Measurement of gain and saturation parameters of a single-mode Yb: silica fiber amplifier," *Optical Fiber Technology*, vol. 19, pp. 446-455, 2013.